Thermochimica Acta 485 (2009) 43–48

Contents lists available at ScienceDirect

Thermochimica Acta

journal homepage: www.elsevier.com/locate/tca

Glass transition in thermosetting clay-nanocomposite polyurethanes

C. Esposito Corcione*, A. Maffezzoli

Dipartimento di Ingegneria dell'Innovazione, Università del Salento, Via Monteroni 73100, Lecce, Italy

ARTICLE INFO

Article history:
Received 19 June 2008
Received in revised form 3 December 2008
Accepted 6 December 2008
Available online 13 December 2008

Keywords:
Nanocomposites
Polyurethanes
Rigid amorphous fraction

ABSTRACT

In this work nanocomposite in a polyurethane (PU) matrix, using an organically modified montmorillonite (OMM), were studied. An amount of organoclay ranging from 2% up to 6% by volume was added to the polyol component of the resin before mixing with isocyanate.

The basal distance of OMM before and after mixing with the polyol and after curing was characterized by X-ray diffraction. The glass transition temperature (T_g) of PU nanocomposites, measured using differential scanning calorimeter, increases with increasing the volume fraction of OMM. On the other hand, the heat capacity increment, ΔC_p, decreases from that the unfilled PU to that of the sample with 5.7 vol.% of OMM. Therefore the rigid amorphous fraction of the PU nanocomposites increases with increasing volume fraction of OMM. Finally, a three-phase model similar to that applied to study semi-crystalline polymers, was used to analyze the intercalation of the PU chains between OMM lamellae. The definition of molecular cooperativity was discussed for these systems and the characteristic length of the cooperative region was determined, using Donth equation.

1. Introduction

Polyurethanes (PUs) are unique polymeric materials with a wide range of physical and chemical properties with applications as coatings, adhesives, fibre, foams and elastomers [1]. Since polyurethane/clay-nanocomposite was introduced by Wang and Pinnavia [2], many polyurethane/clay-nanocomposite have been proposed [3–8]. In contrast to microcomposites, impressive improvements in performance were achieved with a small amount of filler. This was ascribed to the high aspect ratio of the exfoliated clay layers. The most studied nanocomposites are composed of thermoplastic or thermosetting matrix and an organically modified montmorillonite (OMM) [9–13]. Natural montmorillonite consisted of layers made up of two silicate tetrahedron fused to an edge-shared octahedral sheet of either aluminium or magnesium hydroxide. The physical dimensions of these platelet-like shaped silicate layers were typically of about 100 nm in diameter and 1 nm in thickness. Isomorphic substitution within the layers generates negative charges that are normally counter-balanced by cations (Na^+, Ca^{2+}, K^+) residing in the interlayer galleries space [14]. Since momtmorillonite is hydrophilic and it is characterized by a poor affinity with hydrophobic organic polymers, organic cations such as alkylammonium cations are used to change the originally hydrophilic silicate interlayer spacing into a hydrophobic surface. The organic cations lower the surface energy of silicate layers and enhance the miscibility between the silicate layers and the polymer matrix [15–19].

In this work nanocomposite obtained using an organically modified montmorillonite in a polyurethane matrix was synthesized and characterized. The microstructure of the composites was investigated by X-ray diffraction. The glass transition temperature T_g of PU nanocomposites, was measured together with the heat capacity increment, ΔC_p, using differential scanning calorimeter (DSC). The rigid amorphous fraction (RAF) of the PU nanocomposites was calculated and it increases with increasing volume fraction of OMM. The intercalation of the PU chains between OMM lamellae was analyzed, using a three-phase model similar to that applied to study semi-crystalline polymers. A possible definition for the molecular cooperativity region of PU nanocomposites was given and the flocculation formula of Donth [20] was used in order to determine the characteristic length of the cooperative region.

2. Experimental

2.1. Materials

The organoclay, supplied by Laviosa (Livorno, Italy), are commercially available as Dellite HPS and Dellite 43B. Dellite HPS is a purified unmodified natural montmorillonite, while Dellite 43B is a OMM derived from natural montmorillonite especially purified and modified with a high content of dimethyl benzylhydrogenated tallow ammonium salt.

A two-component aromatic polyester-based polyurethane adhesive consisting of a pre-polymer and 60% solution of an

* Corresponding author. Tel.: +39 0832 297326.
E-mail address: carola.corcione@unile.it (C.E. Corcione).

0040-6031/$ – see front matter © 2008 Elsevier B.V. All rights reserved.
doi:10.1016/j.tca.2008.12.009

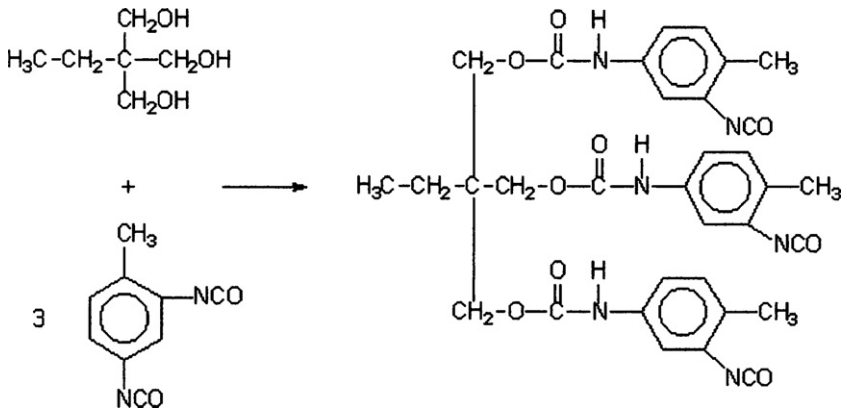

Scheme 1. Structural formula of the aromatic isocyanate TDI/TMP, Polurene FP 75.

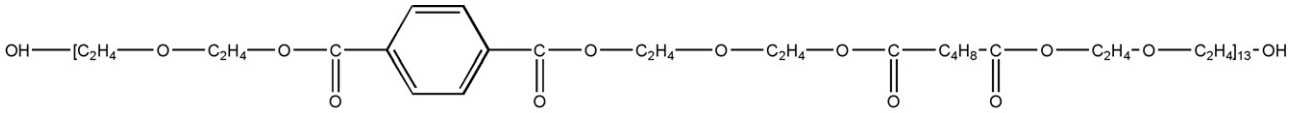

Scheme 2. Structural formula of the polyol Polurene FP 28A.

aromatic polyester polyol in ethyl acetate were used. The crosslinker, Polurene FP 75 (see Scheme 1) consisted of an aromatic isocyanate TDI/TMP (toluene diisocyanate–trimethylpropane). The polyol Polurene FP 28A is a copolymer of isophthalic acid and di-ethylene glycol of an average molecular weight of 6600. The expected chemical formula is shown in Scheme 2. Polurene FP 28A and FP 75 are the components of a solvent-based adhesive currently used for flexible food packaging and technical laminates. The density of the PU matrix reported on data sheet is 1.1 g/cm^3.

2.2. Nanocomposite preparation

Nanocomposites were obtained through in situ intercalative polymerization method [21]. This method consists of five steps:

- Mixing of organoclay and polyol Polurene FP 28A for 1 h at 30 °C in a Haake reomix 600/610, with a mixing velocity = 60 rpm.
- Polyol drying by ethyl-acetate solvent evaporation during mixing.
- Mixing of isocyanate Polurene FP 75 diluted with ethyl-acetate.
- Coating a glass slab with an uniform (0.4–0.6 mm) layer of the polyol–organoclay–isocyanate solution.
- Curing of nanocomposite for 1 week at room temperature (about 25 °C).

FTIR spectra indicated that these curing conditions lead to complete disappearance of peaks associated with the isocyanate group. This confirmed that the cure was complete.

2.3. Characterization techniques

- Wide angle X-ray diffraction (WAXD) were collected on a PW 1729 Philips, using Cu Kα radiation in reflection mode (λ = 0.154 nm). The samples were step-scanned at room temperature from $2\theta = 1.3$–10° in order to determine the d-spacing of organoclay, polyol–OMM systems and nanocomposites. The samples were held in the diffractometer using a socket glass sample holder.
- Glass transition temperature (T_g) of PU nanocomposites was measured using differential scanning calorimeter (DSC METTLER 622 Toledo). Dynamic scans have been ran between −100 and 50 °C at 10 °C/min under nitrogen atmosphere. The samples were analyzed by DSC after curing (performed at room temperature and hence above T_g) cooling the samples down to −100 °C at 10 °C/min. Measurements were performed using samples of about 20 mg. The instrument was calibrated with indium and zinc for temperature and enthalpy measurements, and with sapphire for specific heat measurement, using a heating rate of 10 °C/min. The DSC experiments were repeated at least three times to check the repeatability of results.

3. Results and discussion

3.1. Organofiller characterization

The X-ray diffraction patterns of unmodified and modified montmorillonite samples are reported in Fig. 1. The higher d-spacing for Dellite 43B is attributed to the exchange of the small Na^+ cations with the large organic cations. The larger interlayer spacing coupled with the hydrophobic nature of the organic cations can promote OMM intercalation during mixing with the polymer [4].

The d-spacing of montmorillonite layers is not the only factor which can affect intercalation during mixing with the polymer. In

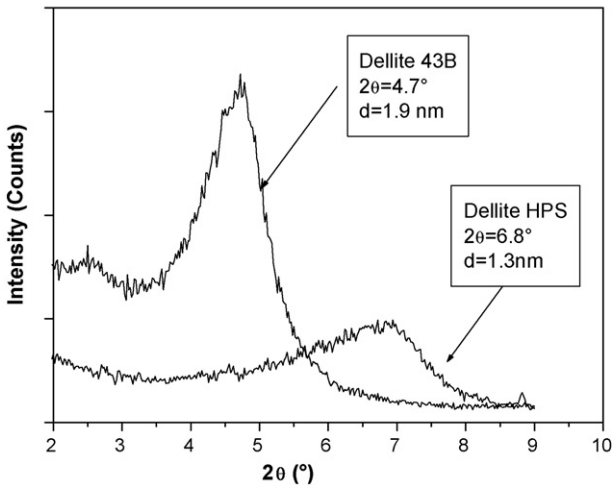

Fig. 1. X-ray diffraction patterns of unmodified and modified montmorillonite.

Table 1
Physical properties of Dellite 43B and Dellite HPS.

Sample	Volume fraction of organic content x_{org} (%)	2θ	d-Spacing (nm)
HPS	0	6.8°	1.3
43B	28.9	4.7°	1.9

fact, the alkylammonium cations can provide functional groups that can react with the polymer matrix [4]. However in this case only dispersion forces and intermolecular interaction between the polyol segments and the alkylammonium tail can occur.

The volume fraction of the Dellite 43B dispersed at first in the polyol and after in the PU polymer was also determined from thermogravimetric analysis as described elsewhere [21] and reported in Table 1.

3.2. Polyol–OMM mixtures

A comparison between the X-ray diffraction patterns of Dellite 43B and the nanofilled polyol obtained by mixing intercalation with Dellite 43B is reported in Fig. 2.

XRD patterns of samples filled with 2.1, 4.2 and 5.7 vol.%, clearly show that the original peak of silicate Dellite 43B is shifted to angle smaller than $2\theta = 1.3°$ (corresponding to d-spacing > 6.7 nm). This suggests that the organoclay, during mixing with the polyol, was at least intercalated with a lamellar spacing higher than 6.7 nm or it was exfoliated.

The sample filled with 7.1 vol.% of OMM shows a peak centered at about $2\theta = 2.4°$, corresponding to a d-spacing of 3.68 nm. This indicates that the OMM was intercalated during mixing, but intercalation is less efficient than in the case of samples filled with a higher content of OMM. Nevertheless, the presence of exfoliated OMM even in this sample, cannot be excluded.

3.3. Polyol nanocomposite crosslinking

3.3.1. XRD

The viscosity of the polyol nanocomposite was reduced adding ethyl acetate and then the isocyanate curing agent. Curing was performed at room temperature for 1 week. The basal distances of crosslinked PU nanocomposites, obtained by X-ray diffraction are reported in Fig. 3.

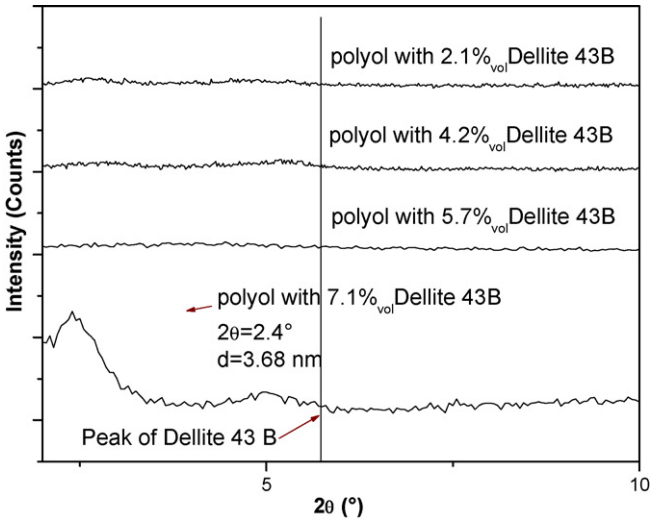

Fig. 2. X-ray diffraction patterns of Dellite 43B and polyol filled with different concentration of the same nanofiller.

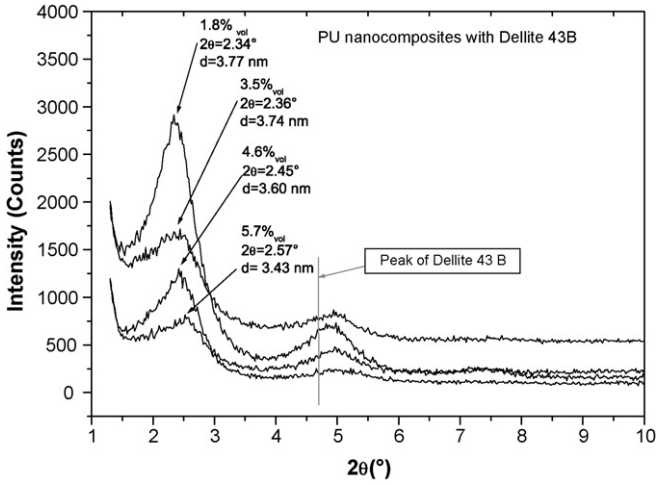

Fig. 3. XRD patterns of PU nanocomposites with 43 B.

The comparison between XRD spectra of Figs. 2 and 3 obtained on the polyol and on the crosslinked polyurethane, respectively shows a reduction of basal distance, even if it is still higher than that of neat OMM. Diffraction peaks at higher angles indicate that the addition of the solvent and isocyanate decreases the lamellar spacing. The higher affinity of polyol toward ethyl acetate with respect to ammonium salts is likely to determine its extraction from the OMM interlamellar galleries, resulting in a d-spacing decrease [21].

3.4. Rigid amorphous fraction

The glass transition temperature T_g of PU nanocomposites was measured using differential scanning calorimeter as half step temperature. The values of T_g as function of the Dellite 43B content in the polyurethane matrix are reported in Table 2. The corresponding specific heat (C_p) change, calculated as the step height, is shown in Fig. 4. For one of the samples the dotted line reported in Fig. 4 represents the uncertainty range. T_g increases from 238 K for the unfilled polyol (as reported in a previous work [21]) to 241 K for the crosslinked polyurethane. Increasing the OMM content, T_g reaches 254.2 K for the sample with 5.7 vol.% of Dellite 43B. On the other hand, the change at T_g of heat capacity, ΔC_p, normalized to the weight of the organic fraction, given by PU and organic modifier, decreases from 1.02 J/g K for the unfilled polyol to 0.74 J/g K for the sample with 5.7 vol.% of Dellite 43B. Therefore a rigid amorphous fraction x_{ra} [22,23] can be calculated as the ratio between

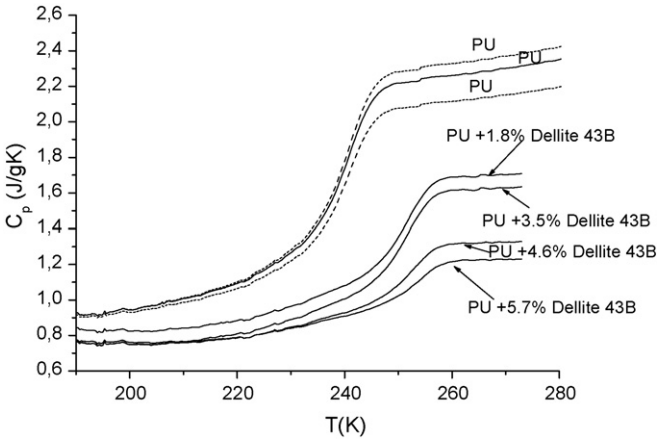

Fig. 4. Comparison between C_p curves of unfilled PU with PU filled with Dellite 43B.

Table 2
Thermal parameters of all samples of nanocomposites and cooperativity length ξ_α calculated from Donth equation.

PU with vol.% Dellite 43B	T_g (K)	ΔC_p (J/g K) Normalized to PU and organic modifier weight	x_{ra}	ΔT (K)	ξ_α (nm) from Eq. (2)	ξ_α (nm) from Eq. (3)
0	241 ± 4.8	1.02 ± 0.09	0	15.89 ± 0.032	1.1 ± 0.08	1.7 ± 0.13
1.8	248.6 ± 4.5	0.88 ± 0.081	0.14 ± 0.01	15.01 ± 0.022	1.3 ± 0.11	2.1 ± 0.17
3.5	251.9 ± 5.2	0.80 ± 0.09	0.22 ± 0.02	15.13 ± 0.04	1.3 ± 0.10	2.1 ± 0.15
4.6	252.9 ± 2.8	0.79 ± 0.053	0.23 ± 0.009	15.21 ± 0.07	1.3 ± 0.12	2.1 ± 0.19
5.7	254.2 ± 5.2	0.74 ± 0.09	0.28 ± 0.06	17.37 ± 0.05	1.2 ± 0.07	1.9 ± 0.15

the change of heat capacities of filled PU $\Delta C_p(f)$ to that of unfilled one, $\Delta C_p(u)$:

$$x_{ra} = 1 - \frac{\Delta C_p(f)}{\Delta C_p(u)} \quad (1)$$

The values of x_{ra} calculated with Eq. (1) are also reported in Table 2 and in Fig. 5. The rigid amorphous fraction of the PU nanocomposites increases with increasing volume fraction of Dellite 43B. As shown in Fig. 4 the segmental mobility is significantly reduced as OMM increases indicating that chains immobilization occurs when they are intercalated between OMM lamellae. This behavior can be compared to those of semi-crystalline polymer where a rigid amorphous fraction is typically observed [24–29]. Similarly OMM lamellae can act as lamellar chain folded crystals presenting polymer molecules partially immobilized and even bridging two OMM stacks. This possible interpretation indicates that even in the polyol this is likely to occur: large rheological units made of OMM lamellae and polymer chains partially or totally intercalated are generated. OMM are able to bridge a larger number of OMM lamellae as the filler weight fraction increases, leading to a corresponding high viscosity of the OMM/polyol nanodispersion. These large units behaving as an entangled polymer of very high molecular weight are responsible of the strong non-Newtonian behavior of the filled polyols, as reported in a previous work [21].

Two competing models exist to describe the organization of the lamellae of a semi-crystalline polymer within the spherulites, i.e., the Heterogeneous Stack Model, HET [30], and the Homogeneous Stack Model, HSM [31], as shown in Fig. 6. The nature of the lamellar structure, whether lamellae are space filling or not, determines whether the HET or HSM is appropriate for a given polymer. HET makes the assumption that the entire mobile amorphous region (MAF) is outside the lamella stacks and the rigid amorphous fraction is the only amorphous material located between adjacent lamellae. The authors assume that the amorphous or non-crystalline species between chain folded lamellae crystals do not contribute to the glass transition. Their results on semi-crystalline polymers suggest that the conventionally measured glass transition originate from the broad amorphous gaps in the space-filling spherulitic systems [30]. On the other hand, in the HSM, the mobile amorphous region is supposed to be inside the chain folded crystals stacks and the rigid amorphous material is an interfacial layer between the crystals and the MAF. Direct observation of the crystal–amorphous interphase in the polymer investigate, obtained by the authors using AFM analysis, seems to indicate that the entire intra-lamellar amorphous phase should be considered as rigid [31]. In both models, it is supposed the presence of a glass transition cooperativity region, with a characteristic length, generally indicated as ξ_α [20]. The existence of cooperativity rearranging regions (CRR) (for example spheres of radius ξ_α or cubes of length ξ_α) is a basic concept in several theories and models of glass transition [20,32–34]. Basically it means that the rearranging movement of one particle is only possible if a certain number (i.e., N_α = number of molecules or monomeric units of polymers) of neighbor particles is also moved [19]. The molecules do not relax independently of one another and that the motion of a particular molecule depends to some degree on that of its neighbors. This leads to rearrangements of all N_α particles, with possible four conditions [20]:

1. The rearranging movement of the neighbors does not need to occur simultaneously in the strict meaning of the words, but at least some causal sequence is needed.
2. The rearranging path of each molecule has local random kinks, i.e., of order one molecule diameter, and the paths of different particles are different with random events.
3. The rearranging movements corresponding to a certain dispersion zone are considered to be independent from movements corresponding to another dispersion zone.
4. The probability of molecular fluctuations of a cooperativity rearranging regions, having a volume V_α containing N_α particles, is controlled by only the Boltzmann constant (k_B) and the temperature (T) for the whole region.

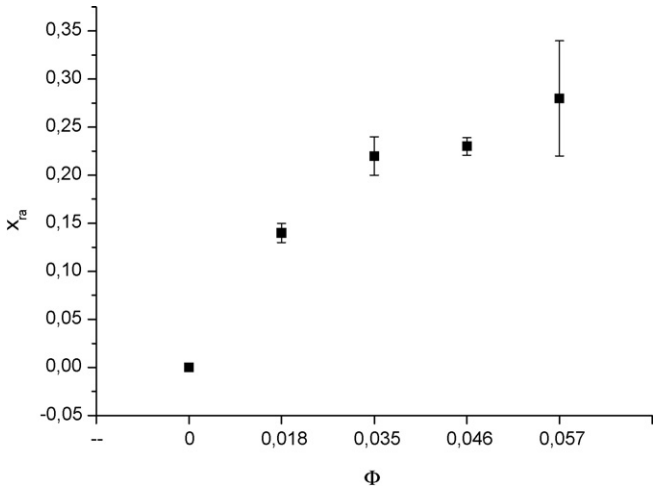

Fig. 5. Rigid amorphous fraction, x_{ra} as function of volume fraction of Dellite 43B.

The size of a cooperativity rearranging regions is defined by as a subsystem of the sample, which, upon a sufficient fluctuation in energy, can rearrange into another configuration independently of its environment. The characteristic length of glass transition, ξ_α is a property of the kinetic structure that can be defined as the cube root of the volume of the molecular cooperativity region, V_α. Assuming that cooperativity rearranging regions are spheres of radius ξ_α [20], the characteristic length can be obtained by Eq. (2):

$$\xi_\alpha = \sqrt[3]{\frac{V_\alpha}{4\pi} \times 3} \quad (2)$$

Supposing that CRR are cubes of side ξ_α, the characteristic length can be obtained by Eq. (3) [22]:

$$\xi_\alpha = \sqrt[3]{V_\alpha} \quad (3)$$

Assuming that the local rearranging mobility is controlled by local density (or, in other words, by local free volume), ξ_α can be connected with a typical length scale of the pattern for spatial and

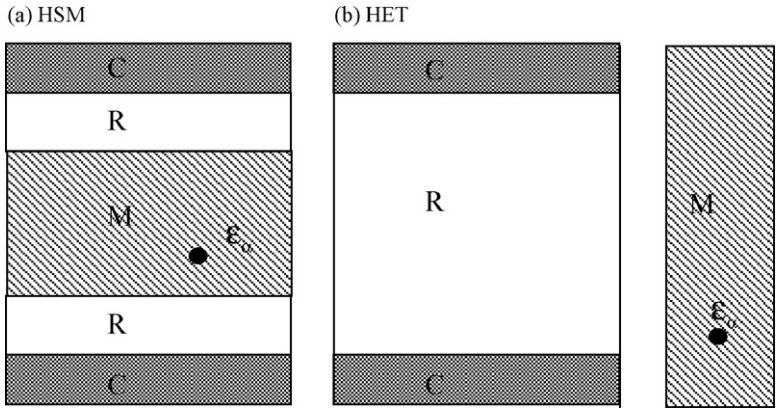

Fig. 6. Schematic representation of two structural models for semi-crystalline polymers exhibiting lamellar structure: crystal lamella (C), rigid amorphous layer (R), and mobile amorphous layer (M).

temporal density fluctuation. Starting from Einstein's fluctuation formula for the probability of molecular fluctuation of a subsystem, Donth derived a fluctuation formula in order to calculate the characteristic length of the cooperativity region [20]:

$$V_\alpha = \frac{k_B T_g^2 \Delta(1/C_v)}{(\delta T)^2 \rho} = \frac{4}{3}\pi\xi_\alpha^3 \quad (4)$$

where C_v is the specific heat at constant volume and ρ is the mass density of the bulk. δT represents the mean temperature fluctuation of one α functional subsystem of size V_α. Donth suggests some approximations to simplify the use of Eq. (4) for the calculation of ε_α. First heat capacities at pressure and volume constant are assumed equal (i.e., $C_p \cong C_v$). This approximation usually has an uncertainty smaller than 10% since the smaller $\Delta C_v < \Delta C_p$ values are partially compensated by C_v/C_p <1. Using this approximation, the step height $\Delta C_v^{-1} \cong \Delta C_p^{-1}$, can be directly determined from DSC thermograms following the procedure suggested by Huth et al. [35]:

$$\Delta C_p^{-1} \approx \frac{\Delta C_p}{\bar{C}_p^2} \quad (5)$$

where $\bar{C}_p = (C_p^l + C_p^g)/2$ is the average between glass (C_p^l) and liquid (C_p^g) heat capacities.

Substituting Eq. (5) in Eq. (3), V_α can be expressed as

$$V_\alpha = \frac{4k_B T_g^2 \Delta C_p}{(C_p^l + C_p^g)^2 (\delta T)^2 \rho} = \frac{4}{3}\pi\xi_\alpha^3 \quad (6)$$

The second approximation suggested by Donth [20] leads to estimate the mean temperature fluctuation from the width of the glass transition step ΔT as $\delta T \cong 0.4\Delta T$. To check this procedure for the calculation of the characteristic length, Donth [20] looked for a series of polymers where a large variation of this length should be expected. Typical values for polymers at T_g are ξ_α = 2–3 nm and N_α = a few hundred monomeric units. However the ξ_α values calculated using Eq. (3) from Donth [20] can only be considered a rough estimations, because this method is affected by systematic errors, mainly due to the uncertainties of the tangent construction for C_p^l and C_p^g [20].

Recently, large amount of polymer/layered silicate nanocomposites were prepared ant its related physical and chemical phenomena, such as molecular confinement have been investigated [36–38]. Nano-sized spaces including nanopore and nanolayer provide the opportunity to identify the characteristic length the amorphous matrices. Many studies based on nanopore and nanoscaled polymers have been made [39–42]. Calorimetric experiments on a wide assortment of molecular glass formers confirmed that the characteristic length of the cooperativity region near T_g is typically 1.0–3.5 nm and it is affected by individual properties of the molecules [11]. However more evidences are still needed for crosslinked polyester polyurethanes in the presence of nanostructured fillers such as OMM.

In this paper, the characteristic length of PU nanocomposites was calculated, assuming that the immobilization of PU linear segments between OMM lamellae presents a similar behavior to the semi-crystalline polymers. Since the interaction between PU chains and the organic modifier involve mainly dispersive and polar forces, it is likely that the HET model is better suitable for these amorphous matrix nanocomposites. The binding energy at the external surfaces of delaminated clay lamella is weak and it should affect only in a limited way the PU chain mobility at T_g. A schematic representation of HET model for PU–OMM nanocomposites is reported in Fig. 7.

According to Donth [20], ξ_α can be calculated from thermal analysis of the T_g, assuming that the cooperativity rearranging regions is spherical, using Eq. (2) or is cubic, using Eq. (3). The thermal parameters of all samples of nanocomposites and cooperativity length ξ_α calculated from Eqs. (2) and (3) are reported in Table 2. The values of ξ_α reported in Table 2 are of the same order of those formed for other semi-crystalline polymers [26] and for other clay nanocomposites [11]. ξ_α has a very limited change when OMM is added to the PU. This could be associated with the presence in the nanocomposite of free chain segments and of freezed molecules. The former are influenced by the presence of OMM showing ξ_α values equal to those of neat PU. The last are intercalated chain segments completely immobilized and responsible of the rigid amorphous free chain of Fig. 5. These results indicates that HET model is more suitable to explain the behavior of these nanocomposites at T_g. The

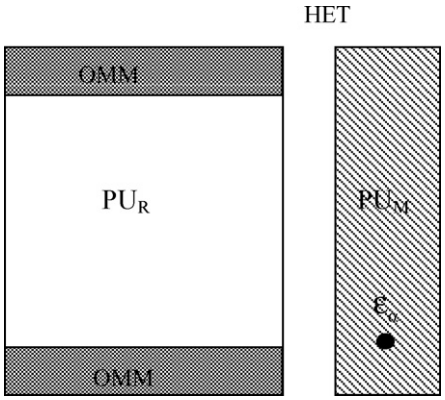

Fig. 7. Schematic representation of the structural model HET for PU-OMM nanocomposites: rigid polyurethane (PU_r), mobile polyurethane (PU_M), and organically modified montmorillonite (OMM).

higher T_g can be explained assuming that the nano-dispersed filler is responsible of higher energy barrier to chain mobility but it does not limit the size of CRR.

4. Conclusion

Nanocomposite adhesives obtained using a montmorillonite, modified with organic cations, in a polyurethane matrix were synthesized and characterized. A mix of exfoliated and intercalated layers was observed in all composites according to the structural and macroscopic properties of the nanocomposites. A significant increase of T_g of nanocomposites with OMM content was also observed, confirming the good dispersion of the nanofiller. The intercalation of polyester polyol between OMM lamellae was easily achieved by mixing. The presence of a significant fraction of rigid amorphous was revealed by calorimetric analysis. In analogy with the interpretation of rigid amorphous fraction used for semi-crystalline polymers the Heterogeneous Stack Model was considered closer to the behavior of these nanocomposites. Furthermore a substantially constant value of the characteristic size of the cooperativity rearranging region at T_g was calculated.

Acknowledgement

This work has been funded by Italian government under the project Prin 04 “Polyurethane based adhesives and coatings for flexible packaging modified with nanofillers”.

References

[1] K. Byung Kyu, J.W. Seo, H.M. Jeong, Eur. Polym. J. 39 (2003) 85.
[2] Z. Wang, T.J. Pinnavia, Chem. Mater. 10 (12) (1998) 3769.
[3] C. Zilg, R. Thomann, R. Mulhaupt, J. Adv. Mater. 11 (1) (1999) 49.
[4] K.J. Yao, M. Song, D.J. Hourston, D.Z. Luo, Polymer 43 (3) (2002) 1017.
[5] T.K. Chen, Y.I. Tien, K.H. Wei, J. Polym. Sci. Polym. Chem. 37 (13) (1999) 2225.
[6] T.K. Chen, Y.I. Tien, K.H. Wie, Polymer 41 (4) (2000) 1345.
[7] Y.I. Tien, K.H. Wie, Polymer 42 (7) (2001) 3213.
[8] Y.I. Tien, K.H. Wie, Macromolecules 34 (26) (2001) 9045.
[9] S. Komarneni, J. Mater. Chem. 2 (1992) 1219.
[10] H. Gleiter, Adv. Mater. 4 (1992) 474.
[11] B.M. Novak, Adv. Mater. 5 (1993) 422.
[12] R.F. Ziolo, E.P. Giannelis, B.A. Weinstein, M.P. O'Horo, B.N. Granguly, V. Mehrota, M.W. Russel, D.R. Huffman, Science 257 (1992) 219.
[13] F. Bauera, H.-J. Glasela, E. Hartmanna, H. Langgutha, R. Hinterwaldner, Int. J. Adhes. Adhes. 24 (2004) 519.
[14] L. Torre, E. Frulloni, J.M. Kenny, C. Manferti, G. Camino, J. Appl. Polym. Sci. 90 (2003) 2532.
[15] K. Yano, A. Usuki, A. Okada, T. Kurauchi, O. Kamigaito, J. Polym. Sci. A: Polym. Chem. 31 (1993) 2493.
[16] As. Moet, A. Akelah, Mater. Lett. 18 (1993) 97.
[17] L.P. Meier, R.A. Shelden, W.R. Caseri, U.W. Suter, Macromolecules 27 (1994) 1673.
[18] M.W. Noh, D.C. Lee, Polym. Bull. 42 (1999) 619.
[19] F. Dietsche, R. Mullaupt, Polym. Bull. 43 (1999) 395.
[20] E. Donth, J. Polym. Sci. B 34 (1996) 2881.
[21] C. Esposito Corcione, P. Prinari, D. Cannoletta, G. Mensitieri, A. Maffezzoli, Int. J. Adhes. Adhes. 28 (2008) 91.
[22] C. Schick, E. Donth, Phys. Scr. 43 (1991) 423.
[23] B. Hahn, J. Wendorff, Macromolecules 18 (1985) 718.
[24] X. Lu, P. Cebe, Polymer 37 (1996) 4857.
[25] S. Iannace, A. Maffezzoli, G. Leo, L. Nicolais, Polymer 42 (2001) 3799.
[26] H. Xu, P. Cebe, Macromolecules 37 (2004) 2797.
[27] A. Minakov, D. Mordvintsev, R. Tol, C. Schick, Thermochim. Acta 442 (2006) 25.
[28] A. Saiter, N. Delpouve, E. Dargent, J.M. Saiter, Eur. Polym. J. 43 (2007) 4675.
[29] N. Delpouve, A. Saiter, J.F. Mano, E. Dargent, Polymer 49 (2008) 3130.
[30] B.B. Sauer, B.S. Hsiao, Polymer 36 (13) (1995) 2553–2558.
[31] C. Alvarez, I. Sics, A. Nogales, Z. Denchev, S.S. Funari, T.A. Ezqurra, Polymer 45 (2004) 3953.
[32] C. Schick, E. Donth, Phys. Scr. 43 (1991) 423–429.
[33] J. Dobbertin, A. Hensel, C. Schick, J. Therm. Anal. Calorim. 47 (1996) 1388.
[34] G. Adams, J.H. Gibbs, J. Chem. Phys. 43 (1965) 139.
[35] H. Hunth, M. Beiner, S. Weyer, M. Merzlyakov, C. Schick, E. Donth, Thermochim. Acta 377 (2001) 113.
[36] S.S. Ray, M. Okamoto, Prog. Polym. Sci. 28 (2003) 1539.
[37] K.J. Yao, M. Song, D.J. Hourston, D.Z. Luo, Polymer 3 (2002) 1017.
[38] Y.I. Tien, K.H. Wei, Macromolecules 34 (2001) 9045.
[39] E. Hemple, A. Huwe, K. Otto, F. Janowski, K. Schroter, E. Donth, Thermochim. Acta 337 (1999) 81.
[40] H. Xia, M. Song, Thermochim. Acta 429 (2005) 1.
[41] J. Jin, M. Song, K.J. Yao, Thermochim. Acta 447 (2006) 202.
[42] A. Sargsyan, A. Tonoyan, S. Davtyan, C. Schick, Eur. Polym. J. 43 (2007) 3113.